Nonequilibrium thermodynamics of dilute polymer solutions in flow

Folarin Latinwo,[1] Kai-Wen Hsiao,[1] and Charles M. Schroeder[1,2,3,a)]
[1]*Department of Chemical and Biomolecular Engineering, University of Illinois, Urbana, Illinois 61801, USA*
[2]*Department of Materials Science and Engineering, University of Illinois, Urbana, Illinois 61801, USA*
[3]*Center for Biophysics and Computational Biology, University of Illinois, Urbana, Illinois 61801, USA*

(Received 13 June 2014; accepted 21 October 2014; published online 6 November 2014)

Modern materials processing applications and technologies often occur far from equilibrium. To this end, the processing of complex materials such as polymer melts and nanocomposites generally occurs under strong deformations and flows, conditions under which equilibrium thermodynamics does not apply. As a result, the ability to determine the nonequilibrium thermodynamic properties of polymeric materials from measurable quantities such as heat and work is a major challenge in the field. Here, we use work relations to show that nonequilibrium thermodynamic quantities such as free energy and entropy can be determined for dilute polymer solutions in flow. In this way, we determine the thermodynamic properties of DNA molecules in strong flows using a combination of simulations, kinetic theory, and single molecule experiments. We show that it is possible to calculate polymer relaxation timescales purely from polymer stretching dynamics in flow. We further observe a thermodynamic equivalence between nonequilibrium and equilibrium steady-states for polymeric systems. In this way, our results provide an improved understanding of the energetics of flowing polymer solutions. © *2014 AIP Publishing LLC*. [http://dx.doi.org/10.1063/1.4900880]

I. INTRODUCTION

Classical thermodynamics provides an elegant framework to characterize the properties of a system at equilibrium. In nature, however, biological processes often occur far from equilibrium. Moreover, industrial processing of complex materials such as polymer melts generally occurs under strong deformations and flows, conditions under which equilibrium thermodynamics likely do not apply. From this perspective, there is a strong need for development of methods that allow for characterization of thermodynamic properties of flowing systems.[1–3]

A wide array of processes such as flow-induced crystallization,[4] fluidic-directed self-assembly,[5] and stress-induced phase separations[6] is governed by a strong interplay between nonequilibrium thermodynamics and flow behavior. Furthermore, fundamental molecular phenomena in soft matter processes determines the emergent macroscopic response and corresponding materials properties. Therefore, it is crucial to develop a molecular-level approach that connects the nonequilibrium energetics of soft materials to transient flow conditions. From this perspective, a molecular-level thermodynamic framework for flowing systems will allow for a fundamental route to understand and design processes governed by thermodynamics and rheology.

The ability to determine the nonequilibrium thermodynamic properties of flowing polymer solutions from measurable quantities such as work is a major challenge in the field.[4,7–10] In prior studies in rheology, nonequilibrium thermodynamics has been used primarily to assess the validity of constitutive models that relate the bulk stress in a suspension or solution to flow behavior.[11] In this way, the GENERIC formalism (general equation for the nonequilibrium reversible-irreversible coupling) was utilized to provide thermodynamically valid descriptions of materials.[12–14] The GENERIC approach allows for probing bulk-level constitutive models in accordance with the second law of thermodynamics. However, this bulk-level approach does not allow for the determination of thermodynamic properties from *dynamic* information that is relevant to molecular rheology and polymer physics.

Recently, a new class of identities known as fluctuation theorems (FTs) and work relations has been developed to analyze transitions between the states of a system.[3,15–19] Jarzynski derived an equality that allows for the determination of equilibrium free energy differences from nonequilibrium work measurements,[18] and Hatano and Sasa derived a related second law for steady-state thermodynamics.[3] In addition to the development of FTs, numerical and experimental investigations have demonstrated the validity of FTs. Several reports have focused on equilibrium steady-states (ESSs),[20–26] though recently, an expression was developed for determining nonequilibrium thermodynamic quantities for systems near-equilibrium.[27]

In this work, we report the direct determination of far-from-equilibrium thermodynamic properties for dilute polymer solutions in flow using a combination of simulations and single molecule experiments. We apply work relations to analyze nonequilibrium steady-states (NESSs) for flowing polymer systems, and we calculate quantities such as free energy and entropy for flowing systems. We show proof-of-principle demonstration of this approach using single DNA molecules in fluid flow, which serves as a model system for molecular rheology and polymer physics. In particular, we consider polymer dynamics in an extensional flow, which displays nonequilibrium phase transition,[7] and is a ubiquitous

a)Electronic mail: cms@illinois.edu

"strong" flow in materials processing that underlies polymer extrusion and injection molding.[28] Overall, this approach uncovers new information regarding the fundamental flow properties of complex fluids, which can be used to study nonequilibrium phase transitions.

II. THEORY

A. Equilibrium and nonequilibrium steady-states for polymers in flow

A polymer can be transitioned between ESSs or NESSs in fluid flow. Recently, a work relation was used to study polymer stretching in hydrodynamic flow, wherein the terminal states are defined as a polymer maintained at a fixed molecular extension, which corresponds to an equilibrium state.[25,26] In the present work, however, the terminal states are defined by a polymer chain maintained at a constant flow rate, which corresponds to a nonequilibrium state and fundamentally distinct compared to transitions between ESSs.[20,21,25,26]

We begin by differentiating between ESSs and NESSs. Consider a classical system in contact with a heat bath at temperature T, such that the evolution of the configuration probability distribution p is described by the Fokker-Planck equation. For such a system at an ESS, the transient and spatial rates of change of the probability distribution function are exactly zero. However, for a NESS, only the time derivative is zero, while the spatial derivative is a non-zero constant. In the context of Langevin systems, an equilibrium steady-state is determined by a control parameter λ, and the probability $p_{ess}(x, \lambda)$ of finding the system in a given configuration x follows a Boltzmann distribution:

$$p_{ess} = \frac{\exp\left[-\beta U\left(x, \lambda\right)\right]}{Z_{ess}}, \tag{1}$$

where $\beta^{-1} = k_B T$ is the Boltzmann temperature, U is the potential energy function of the system, $Z_{ess} = e^{-\beta F}$ is the partition function, and $F(\lambda)$ is the Helmholtz free energy of the equilibrium state (Table I). The choice of the parameter λ defines the equilibrium state; for a polymeric system, λ is chosen as the molecular extension of a polymer chain.

For a nonequilibrium steady-state, however, the distribution function p_{ness} does not generally follow a Boltzmann distribution. The partition function $Z_{ness} = e^{-\beta F^*}$ is not directly related to its Helmholtz free energy, but rather to an effective free energy $F^*(\boldsymbol{\alpha})$, where $\boldsymbol{\alpha}$ is the set of control parameters that define the nonequilibrium steady-state. For polymers in flow, the control parameters may include the flow strength f and the polymer stretch in flow λ, such that $\boldsymbol{\alpha} = \{\lambda, f\}$. Importantly, there is a class of nonequilibrium steady-states such that

$$p_{ness} = \frac{\exp\left[-\beta\left(U + \chi\right)\right]}{Z_{ness}}, \tag{2}$$

where $\chi(x, f)$ is an energy related to a flow potential.[3] In this case, the Helmholtz energy for the steady-state is given simply as (see Appendix A)

$$F = F^* - \langle \chi \rangle. \tag{3}$$

Examples of systems that fall into this class include free-draining polymer solutions in steady potential flows, Hookean (linear) dumbbells in a shear flow, and polymer melts in a weak shear flow.[4,28] Indeed, there are significantly fewer studies involving the analysis of NESSs compared to ESSs.[15] In this work, we use numerical simulations and experiments to determine the free energy of polymer chains transitioning between states of constant flow rate (NESS) based on dynamic data.

B. Free energy and control parameters

In general, the free energy of a given system may be determined as a function of state variables, order parameters, or control parameters.[29] State variables include quantities such as temperature, pressure, volume, or polymer stretch, whereas order or control parameters refer to any general quantity or collection of quantities that can be used to specify the system. For nonequilibrium systems subjected to flow, control parameters include dynamic quantities such as the applied strain rate or applied stress.

At a fundamental level, the determination of equilibrium free energy as a function of state variables allows for the development of equations of state that describe the system. Moreover, the determination of equilibrium (or metastable) free energy as a function of order or control parameters is routinely used to study a wide range of phenomena including equilibrium phase transitions, protein folding, and transport phenomena in cell machinery.[30,31]

The thermodynamic framework of fluctuation theorems and work relations for calculating free energies was developed in the context of control parameters at a fixed temperature.[15,18] On the basis of this development, we determine nonequilibrium free energies as a function of control parameters, in particular, the imposed flow strengths in dilute polymer solutions under extensional flows. Therefore, the nonequilibrium Helmholtz free energies, and related thermodynamic potentials, reported in this work are of the form $F\left(T, \dot{\epsilon}, L\right)$ or $F\left(T, Wi\right)$, where $\dot{\epsilon}$ is the strain rate, which is a measure of the applied flow strength, L is the contour length of the polymer, which is a measure of chain size, and Wi is the Weissenberg number (see Sec. III) that incorporates the effect

TABLE I. Thermodynamic quantities for equilibrium steady-states (ESSs) and nonequilibrium steady-states (NESSs) in potential flows.

Property	ESS	NESS
Steady-state distribution function, p_{ss}	$Z_{ess}^{-1} \exp\left[-\beta U\right]$	$Z_{ness}^{-1} \exp\left[-\beta\left(U + \chi\right)\right]$
Thermodynamic functions	F, $\langle U \rangle$, S	F, $\langle U \rangle$, S, F^*, $\langle \chi \rangle$
Relationship between Helmholtz free energy F and partition function Z	$F = -\beta^{-1} \ln Z_{ess}$	$F^* = F + \langle \chi \rangle = -\beta^{-1} \ln Z_{ness}$

of chain size into the flow strength via the longest polymer relaxation time.

C. Work expression for polymeric systems

In order to investigate the thermodynamics of systems that follow the formalism given by Eq. (2), the Helmholtz free energy must be determined with respect to the set of control parameters $\boldsymbol{\alpha}$. Work relations such as the Jarzynski equality (JE) allow for the determination of Helmholtz free energy differences between ESSs, wherein a system is moved between equilibrium states via nonequilibrium transitions, and repeated measurements of the work are used to determine the free energy changes. A related equality was developed for determining the effective free energy differences between NESSs, however, it requires knowledge of the potential energy function of the system.[3] In this work, we utilize an equality similar in spirit to the Hatano and Sasa relation,[3] albeit one that does not require explicit knowledge or characterization of the potential energy function of the system.

To begin, we follow closely the relation given by Hatano and Sasa,[3] which was derived for equilibrium and nonequilibrium steady-states governed by Langevin dynamics,

$$\left\langle \exp\left[-\int_0^\tau \mathrm{d}t\, \dot{\boldsymbol{\alpha}} \cdot \frac{\partial \phi\,(\mathbf{x};\boldsymbol{\alpha})}{\partial \boldsymbol{\alpha}} \right] \right\rangle = 1, \tag{4}$$

where $\langle \cdot \rangle$ represents an ensemble averaged quantity initialized at steady-state (equilibrium or nonequilibrium), $\phi = -\log p_{ss}\,(\mathbf{x};\boldsymbol{\alpha})$, and p_{ss} is a steady-state probability distribution determined by the set of control parameters $\boldsymbol{\alpha} = \{\lambda, f\}$, and τ is the time required to transition between steady-states given by $\boldsymbol{\alpha}_1$ and $\boldsymbol{\alpha}_2$. Inserting the distribution function p_{ness} for nonequilibrium steady-states into Eq. (4) and considering transitions driven solely by flow f, we obtain

$$\exp(-\beta \Delta F^*) = \left\langle \exp\left[-\beta \int_0^\tau \mathrm{d}t\, \dot{f} \frac{\partial \chi(\mathbf{x}; f)}{\partial f} \right] \right\rangle. \tag{5}$$

Equation (5) allows for the direct determination of the effective free energy difference ΔF^* between NESSs, which is generally not equal to the Helmholtz free energy difference ΔF (Ref. 3). In order to determine the nonequilibrium Helmholtz free energy landscape ΔF from physically measurable quantities, we employ a generalized Jarzynski equality (gJE), such that $\langle e^{-\beta w} \rangle = e^{-\beta \Delta F}$, where w is the work required to transition between states. Importantly, this relation is valid for relating both equilibrium and nonequilibrium steady-states. By inserting Eq. (3) into Eq. (5), we find that the gJE work done on the system in transitioning between two NESSs is given as

$$w = -\Delta \langle \chi \rangle + \int_0^\tau \mathrm{d}t\, \dot{f} \frac{\partial \chi(\mathbf{x}; f)}{\partial f}. \tag{6}$$

In this way, application of the generalized JE to the work expression above allows for the direct determination of the Helmholtz free energy difference between NESSs. We note that the energy χ for polymeric systems in flow is well established from theory.[28] In this present study, χ is a simple function of the imposed flow strength and the polymer conformation (see Appendices B and C).

III. RESULTS AND DISCUSSION

A. Nonequilibrium thermodynamic quantities in flow

Using a combination of Brownian dynamics (BD) simulations[32,33] and single molecule experiments, we studied the response of lambda DNA molecules (48.5 kbp) to transitions between fixed flow rates in planar extensional flow, which consists of an axis of pure fluid compression and an orthogonal axis of pure fluid extension (Figs. 1(a) and 1(b)). In this flow, the fluid velocity is given by $v_x = -\dot{\epsilon} x$ and $v_y = \dot{\epsilon} y$, where x and y are the distances from the fluid stagnation point (point of zero velocity at the origin) along the principal axes of compression and extension, respectively. We define a dimensionless flow strength as the Weissenberg number $Wi = \dot{\epsilon} \tau_R$, defined as the product of the fluid strain rate $\dot{\epsilon}$ and longest polymer relaxation time τ_R. Transitioning a polymer between fixed Wi values in a fluid flow inherently describes transitions between nonequilibrium steady-states in flow.

Simulations of single molecule and ensemble-averaged molecular trajectories for this process are shown in Fig. 1(c), where λ-DNA (48.5 kbp) molecules are transitioned from $Wi_1 = 1$ to $Wi_2 = 1.5$ in extensional flow at rates r spanning two orders of magnitude. BD simulations are based on a free-draining coarse-grained multi-bead-spring model, where polymers are modeled as a series of beads (hydrodynamic drag centers) connected by elastic springs.[34,35] As a consequence, our simulations do not consider intramolecular hydrodynamic interactions (HI) and excluded volume (EV) effects, which are known to be critical for long flexible chains, yet play a fairly insignificant role in the dynamics of short semi-flexible polymer chains such as λ-DNA.[36–38] In both BD simulations and experiments, single polymers are transitioned between fixed flow rates at different transition rates ($r = \mathrm{d}Wi/\mathrm{d}t$), where time t is non-dimensionalized with respect to the characteristic timescale for a Hookean chain, which therefore renders r dimensionless.[39] In all cases, the configuration of the system is allowed to reach steady-state at both initial and final conditions, thereby satisfying the conditions for the generalized JE. The work required for this process is calculated using Eq. (6), and the corresponding nonequilibrium work distributions for different transition rates are shown in Fig. 1(d) (see Appendix C). As expected, the work distribution for the slowest rate ($r = 0.005$) yields the smallest average work and narrowest distribution. Next, we applied the generalized JE to determine the free energy change for this polymer solution under flow. Remarkably, regardless of the irreversibility or energy losses at $r = 0.05$ and $r = 0.5$, the gJE yields the Helmholtz free energy change ($\Delta F = 89.4 \pm 0.1\, k_B T$) between $Wi_1 = 1$ and $Wi_2 = 1.5$.

We also performed a series of single molecule experiments to study the dynamics of fluorescently-labeled λ-DNA molecules in extensional flow (see Appendix D). For these experiments, single DNA molecules are "trapped" near the stagnation point of a planar extensional flow using a feedback-controlled PDMS-based microfluidic device, which enables precise control over the fluid strain rate $\dot{\epsilon}$ with simultaneous center-of-mass confinement during the course of an experiment, as previously reported by our group.[40,41] In one case, we directly observed the dynamics of single λ-DNA

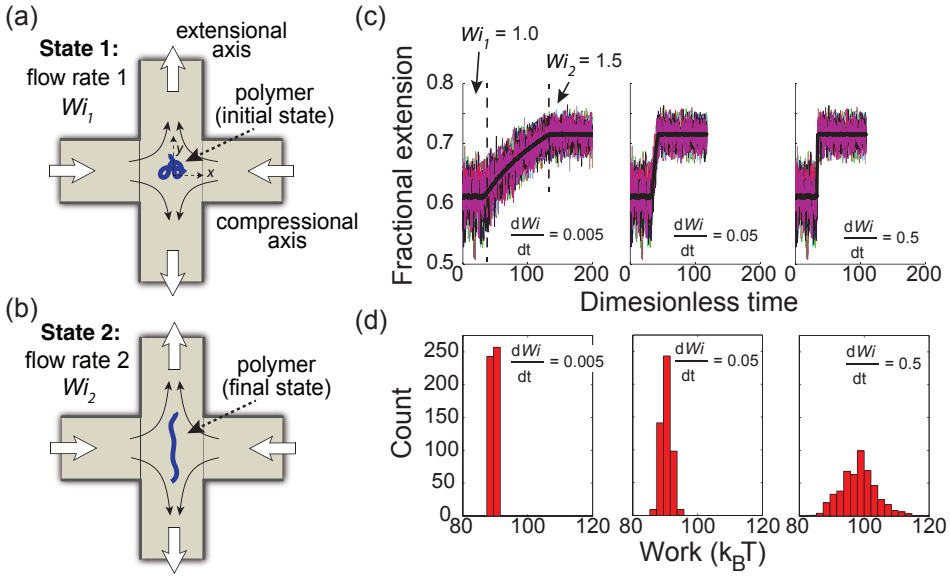

FIG. 1. Nonequilibrium trajectories and work distributions for transitioning single λ-DNA molecules between Wi_1 and Wi_2 in planar extensional flow. (a) and (b) Schematic of single polymer stretching in planar extensional flow from initial state to final state. (c) BD simulations of polymer transitions between $Wi_1 = 1$ and $Wi_2 = 1.5$. Individual trajectories (colored lines) and ensemble-average (black line) of transient trajectories at different transition rates: slow (left panel), intermediate (middle panel), and fast transition rate (right panel). (d) Corresponding work distributions obtained from simulations in (c). For each transition, the simulation ensemble consists of 500 individual molecules.

molecules transitioned between $Wi_1 = 3.0$ and $Wi_2 = 7.3$ at a rate of $r = 3.4$ (Fig. 2(a)). For comparison, we performed corresponding BD simulations under the same conditions, and we find good quantitative agreement between experimental and simulated molecular stretching trajectories (Figs. 2(a) and 2(b), and Fig. S1 in the supplementary material[39]). Next, single molecule trajectories were analyzed using a hydrodynamic model with no free parameters to determine the work done by the fluid on the polymer during a stretching event (see Appendix E). The application of the gJE yields the nonequilibrium Helmholtz free energy change from the stretching process, which was determined to be $\Delta F = 308 \pm 19\ k_BT$ for transitioning between $Wi_1 = 3.0$ and $Wi_2 = 7.3$. For the corresponding simulation, the application of the gJE yields $\Delta F = 343 \pm 1\ k_BT$, which is obtained from a larger ensemble of single molecules compared to experiments (see Fig. S2 in the supplementary material[39]).

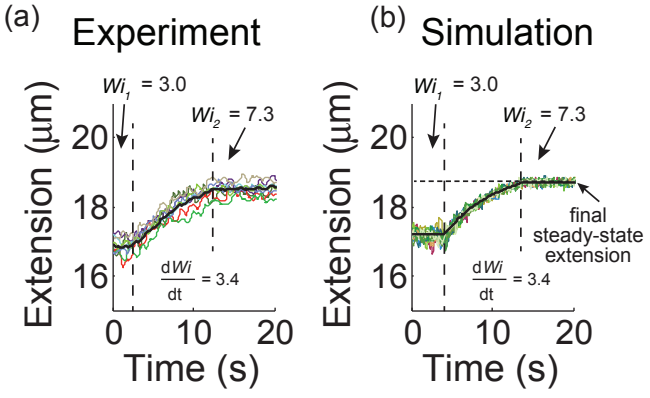

FIG. 2. Molecular stretching trajectories of single DNA chains in planar extensional flow in response to transitions between $Wi_1 = 3.0$ and $Wi_2 = 7.3$ at a transition rate $r = 3.4$ using (a) single molecule experiments and (b) BD simulations. Colored (thin) lines represent individual molecular stretching trajectories, and black (thick) lines represent ensemble-average. The experiment and simulation ensemble consists of 14 and 500 individual molecules, respectively.

We note that, in general, nonequilibrium work distributions are a function of the transition rate r (Fig. 1(d)) and the terminal state points or flow strengths, Wi_1 and Wi_2. To study the effect of the terminal states on work distributions, we constructed a work distribution matrix (WDM) as shown in Fig. 3. This matrix consists of rows that correspond to a fixed initial state, Wi_1, and columns that correspond to a fixed final state ratio, Wi_2/Wi_1. In this way, the elements of the matrix represent the work distribution that corresponds to coordinate $[Wi_1, Wi_2/Wi_1]$ at a specified transition rate.

Using BD simulations, we constructed a 3×5 WDM at a transition rate $r = 0.05$ in planar extensional flow (Fig. 3). We consider three initial states with respect to the coil-stretch transition ($Wi \approx 0.5$). In all cases, we find that the work distributions broaden as one moves from left to right (larger Wi_2 in the final state), or from top to bottom (larger Wi_1 in the initial state) in the WDM. This observation is expected because higher flow strengths result in stretched polymer conformations, which in turn leads to higher energy states and a concomitant broadening in the work distributions.

Surprisingly, in the vicinity of the coil-stretch transition ($Wi_1 = 0.4$, row 2 in Fig. 3), we observe a pronounced skewness of the work distributions that is a strong function of Wi_2/Wi_1. We attribute enhanced skewness of the work distributions in this regime to the fact that the terminal states (Wi_1 and Wi_2) are defined across the coil-stretch transition (see Fig. S3 in the supplementary material[39]). Furthermore, for $Wi_1 = 0.4$, we observe that the skewness of the work distribution is negative for $Wi_2/Wi_1 < 2.0$, and positive for $Wi_2/Wi_1 \geq 2.5$ (see Fig. S4 in the supplementary

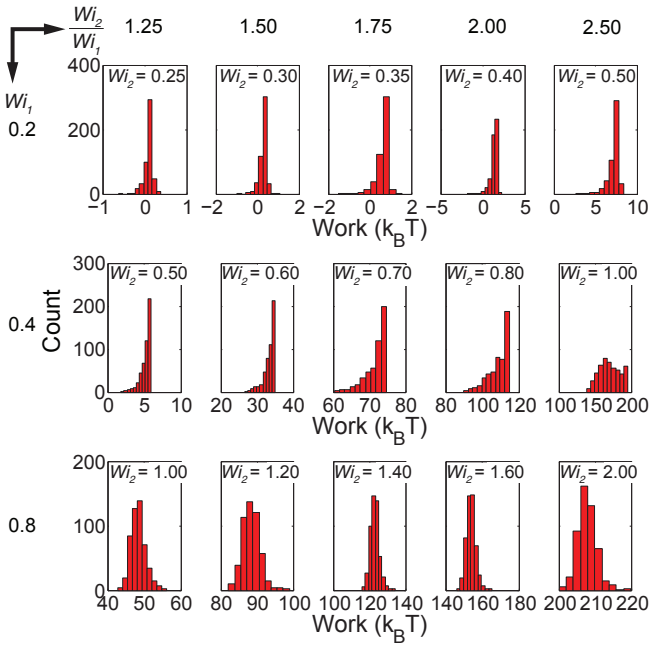

FIG. 3. Work distribution matrix (WDM) for studying the effect of the final state (Wi_2/Wi_1) on nonequilibrium work distributions. Using BD simulations, three initial states were considered ($Wi_1 = 0.2$, 0.4, and 0.8) with five final states for each initial state ($Wi_2/Wi_1 = 1.25$, 1.50, 1.75, 2.0, and 2.5) at a transition rate $r = 0.05$. The WDM reveals both negative and positive skewness (row 2) in the vicinity of the coil-stretch transition.

material[39]). This observation suggests that there exists a critical final state ratio $\left(Wi_2/Wi_1\right)_c$ which corresponds to zero skewness, and beyond which the work distribution is dominated by Wi_2.

For nonequilibrium steady-states in flow, thermodynamic quantities of interest include the effective free energy F^*, a flow energy $-\langle\chi\rangle$, a nonequilibrium Helmholtz free energy F, and a nonequilibrium entropy S. We directly determined these thermodynamic quantities for DNA in extensional flow by transitioning single polymer chains between fixed flow strengths (Fig. 4). First, we determined the effective free energy difference ΔF^* based on the equality provided by Eq. (5), as shown in Fig. 4(a). Moreover, for potential flows such as a planar extensional flow, the flow energy $-\langle\chi\rangle$ can be directly determined from polymer extension in flow (see Appendix C), and this quantity is plotted in Fig. 4(b). Next, the nonequilibrium Helmholtz free energy difference ΔF can be directly determined by the relation given by Eq. (3), or alternatively, by defining the work done by the fluid on the polymer by Eq. (6) and application of the generalized JE. These two approaches are equivalent and yield the nonequilibrium Helmholtz free energy difference ΔF, as shown in Fig. 4(c).

Interestingly, we note that the nonequilibrium Helmholtz free energy F determined from the generalized JE differs significantly from the free energy determined from Marrucci's classic theory,[9] as shown in Fig. 4(c). Similar to this study, Marrucci's theory considers free energies at a fixed velocity gradient or applied strain rate, however, it assumes that the force-extension behavior or equilibrium elasticity of polymer chains is a linear function of extension. Based on this linear assumption, the related nonequilibrium Helmholtz free energy is then directly related to the bulk-level stresses in the flowing polymer solution such that

$$\Delta F = \frac{1}{2}\Delta \mathrm{Tr}(\boldsymbol{\tau}_p), \tag{7}$$

where $\mathrm{Tr}(\cdots)$ represents the trace operation, and $\boldsymbol{\tau}_p$ is the polymer contribution to the stress tensor (see the Appendix material[39]). Nevertheless, we note that the disagreement between the free energy determined from the gJE and the classic theory is expected because the linear equilibrium elasticity assumption fails in strong flows.[28]

The generalized JE approach also allows for determination of the nonequilibrium entropy for flowing polymer systems, as shown in Fig. 4(d). Entropy S was calculated from the relation $F = \langle U\rangle - TS$ (Ref. 3), where the average potential energy $\langle U\rangle$ is evaluated using the stored elastic potential energy of the polymer.[42] Based on the nonequilibrium Helmholtz free energy F, we also calculated a nonequilibrium "elasticity" as $\partial\Delta F/\partial Wi$ as shown in Fig. 4(e). This nonequilibrium elasticity provides a measure of the total thermodynamic resistance of the polymer solution to changes in flow strength. Finally, to connect the nonequilibrium thermodynamic properties to the polymer conformation, we report the steady-state average fractional extension of the polymer as a function of the imposed flow strength as shown in Fig. 4(f).

Strikingly, we found that all of the nonequilibrium thermodynamic quantities show a transition near $Wi \approx 0.5$, which is the location of the coil-stretch transition in extensional flow.[7,8,28,35] For example, flow entropy shows a peak near the coil-stretch transition, which is physically intuitive because entropy is a measure of disorder, and fluctuations in polymer extension are at a maximum near the coil-stretch transition. Our results also show that regardless of the transition rate r, work relations allow for accurate determination of the nonequilibrium thermodynamic properties of flowing systems.

B. Polymer relaxation time from effective free energy

As an application of the nonequilibrium thermodynamic framework for polymers in flow, we demonstrate a new approach to determine the longest relaxation time τ_R for polymers in solution (Fig. 5). In single polymer rheology, the longest polymer relaxation time is generally determined in the absence of flow, however, we were able to determine τ_R from far-from-equilibrium stretching dynamics in flow. For this analysis, consider a single-mode dumbbell model of a polymer, which is appropriate for capturing the stretching dynamics of polymer chains in extensional flow. For a linear dumbbell in extensional flow, kinetic theory predicts that $\Delta F^* = \frac{1}{2}\beta^{-1}\ln[1 - 4Wi^2]$, where $Wi = \tilde{\tau}_R Pe$, $\tilde{\tau}_R$ is the dimensionless relaxation time defined with respect to the characteristic timescale of a Hookean dumbbell, and Pe is the Peclet number (see the supplementary material[39]). By analyzing the near equilibrium regime where $\Delta F^* > -\beta^{-1}$, which corresponds to $Wi < 0.5$ for a Hookean dumbbell, it is possible to determine τ_R by analyzing the effective free energy change ΔF^*.

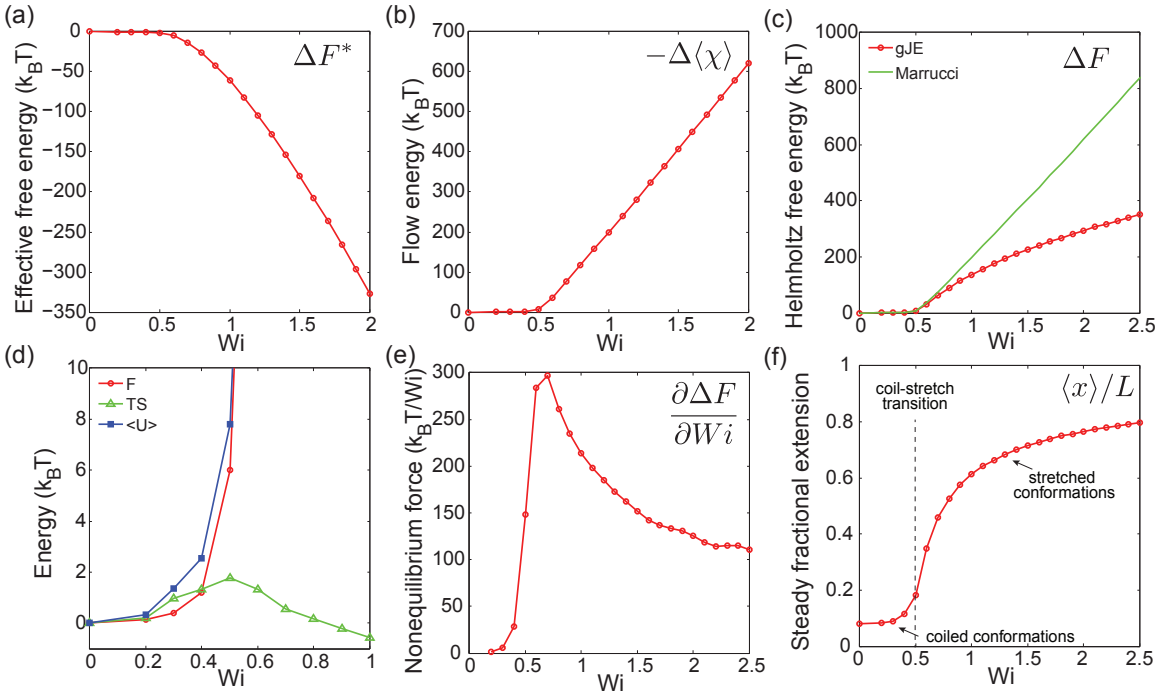

FIG. 4. Nonequilibrium thermodynamic quantities for λ-DNA in a planar extensional flow determined from BD simulations. (a) Effective free energy ΔF^*, (b) flow energy $-\Delta\langle\chi\rangle$, (c) Helmholtz free energy ΔF, (d) energetic contributions in the vicinity of the coil-stretch transition in extensional flow including ΔF, average potential energy, $\Delta\langle U\rangle$, and nonequilibrium entropy, ΔS. (e) Nonequilibrium elasticity in planar extensional flow. The reference state is zero flow, that is, under quiescent conditions ($Wi = 0$). (f) Steady-state fractional extension of λ-DNA in extensional flow determined from BD simulations.

We applied this approach to simulations of multi-bead-spring polymer models,[43] and we determined τ_R for different polymer sizes (Fig. 5). The inset of Fig. 5 shows the effective free energy function used to determine τ_R. The scaling relationship between τ_R and polymer molecular weight is in excellent agreement with Rouse theory,[28] which is expected for free-draining polymers. In addition, we find good quantitative agreement between τ_R determined from the effective free energy under flow conditions, and τ_R obtained from the traditional approach in molecular rheology under no flow conditions (Fig. 5). In this way, we show that polymer relaxation time can be determined using stretching trajectories in flow, whereas traditional approaches prescribe determination of τ_R from an exponential fit to decaying molecular extension trajectories or stress (in the linear regime) following the cessation of flow.[8,28,35]

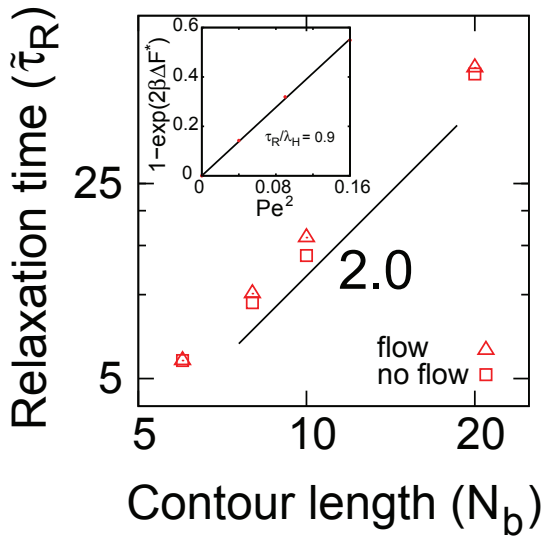

FIG. 5. Relaxation time from effective free energy landscape in flow for different chain sizes (or molecular weights) described by the number of beads, N_b. Longest polymer relaxation time $\tilde{\tau}_R$ for dsDNA is given in terms of the relaxation time for a Hookean dumbbell λ_H. *Pe* is the dimensionless flow strength with respect to the sub-segments of the polymer chain, which is represented by the number of Kuhn segments per spring. The relaxation time under no flow conditions was determined as the time constant obtained from the three parameter exponential fit to the final 30% of chain extension following the cessation of flow. (Inset) General approach for determining relaxation time under flow conditions.

C. Nonequilibrium-equilibrium equivalence in polymeric systems

Finally, we consider the implications of the nonequilibrium thermodynamics approach to ensemble equivalence, which is a central concept in equilibrium thermodynamics. In the thermodynamic limit, it is well known that optical tweezer-based polymer "pulling" experiments carried out under different conditions yield identical results. For example, the properties obtained under a constant-extension protocol (canonical ensemble) are equivalent to those obtained under a constant-force protocol (Gibbs ensemble).[44] Here, we explore the possibility of an ensemble equivalence between nonequilibrium steady-states and equilibrium steady-states in polymeric systems.

Consider the two different polymer systems in the inset of Fig. 6, where the upper panel shows an ESS, defined as a

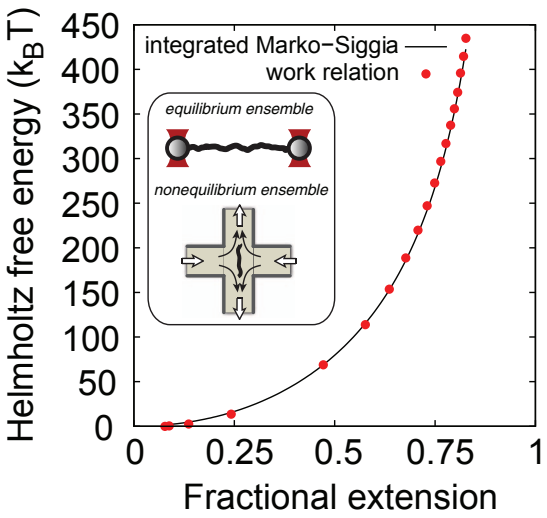

FIG. 6. Equilibrium-nonequilibrium equivalence in polymeric materials. Nonequilibrium Helmholtz free energy landscape for DNA in flow determined from work relations, overplotted with stored elastic energy determined by integrating the Marko-Siggia force-relation. (Inset) Schematic of a polymer molecule held at a fixed extension λ at an equilibrium steady-state (top) and held at a constant flow rate Wi at a nonequilibrium steady-state (bottom).

polymer held at a constant extension λ with a corresponding equilibrium Helmholtz free energy $F_{ess}(\lambda)$. The lower panel shows a NESS, defined as a polymer held at a constant flow strength Wi in an extensional flow with a corresponding nonequilibrium Helmholtz free energy $F_{ness}(Wi)$. We define an equivalence such that the properties of an equilibrium constant extension experiment can be determined from a nonequilibrium experiment at a constant flow strength. Using this approach, we observe the existence of an equilibrium-nonequilibrium equivalence between constant extension and constant flow scenarios in single molecule polymer systems (Fig. 6). In particular, we find that the Helmholtz free energy at a constant extension corresponds to the Helmholtz free energy at a constant flow where the average molecular extension matches the constant extension, such that $F_{ess}(\lambda) = F_{ness}(\langle\lambda\rangle) = F_{ness}(Wi)$. Using this equivalence and recasting F_{ness} as a function of extension, we determine exactly the equilibrium stored elastic energy in the polymer, as shown in Fig. 6. In this way, our work shows that equilibrium properties such as stored elastic energy, and therefore elasticity can be determined from nonequilibrium thermodynamic properties in flowing systems.

IV. CONCLUSION

In this article, we report the determination of nonequilibrium thermodynamic properties for polymers in flow. Our approach utilizes work relations to determine thermodynamic properties based on measurable experimental quantities such as work, whereas the majority of previous studies have focused on the analysis of nonequilibrium thermodynamic potentials using steady-state properties.[4,12,14] The ability to determine the thermodynamic properties of flowing systems from work enables new routes for fundamental analysis of soft condensed matter systems. To this end, we used this approach to calculate the longest polymer relaxation time τ_R, which is a key property of viscoelastic materials traditionally determined from stress relaxation experiments.

The determination of entropy is central to developing a thermodynamic framework for a broad class of systems, including granular materials.[45] In this work, we further report the direct determination of the entropy S of flowing polymeric systems, which may prove useful in understanding flow-induced phase behavior. In addition, we find that the nonequilibrium Helmholtz free energy F determined from the generalized JE differs significantly from the free energy determined from the classic theories.[6,10]

In the context of polymer models, we note that the nonequilibrium thermodynamic properties reported from BD simulations in this study are determined under the free-draining assumption, which is appropriate for short semi-flexible polymer chains such as λ-DNA.[37] However, it is well established that EV effects and intramolecular HI, which represent non-free-draining behavior, can significantly influence the dynamics of long flexible polymer chains. Therefore, we anticipate that HI and EV will have a non-trivial effect on work distributions and corresponding thermodynamic properties of truly long flexible polymer chains in flow; this is subject of future research.

Overall, nonequilibrium thermodynamic quantities provide a powerful platform for analyzing flow-based systems. For example, de Gennes sketched the effective free energy of polymer chains in flow to predict the existence of a conformational hysteresis in extensional flow.[7] Importantly, our work provides a direct quantitative determination of these properties from measurable quantities in flow. With further development, the formalism reported in the present study could be applied to a broad class of soft materials systems including polymer melts and active colloidal systems. In this way, the determination of thermodynamic quantities could ultimately allow for a more fundamental route in the design of polymer processes such as flow-induced crystallization and stress-induced phase separation.[4,6]

ACKNOWLEDGMENTS

We thank Patrick Corona for stimulating discussions, and Dr. Christopher Brockman for initial work on single molecule experiments. This work was supported by a Packard Fellowship from the David and Lucile Packard Foundation and a National Science Foundation (NSF) CAREER Award #1254340 to C.M.S., and a Computational Science and Engineering Fellowship from the University of Illinois to F.L.

APPENDIX A: RELATIONSHIP BETWEEN HELMHOLTZ FREE ENERGY AND EFFECTIVE FREE ENERGY IN POTENTIAL FLOWS

In order to derive the relationship between F and F^* in potential flows, we used the Shannon entropy such that $S = -\int d\mathbf{x} p_{ss} \log p_{ss}$, and the steady-state average potential energy, $\langle U\rangle = \int d\mathbf{x} p_{ss} U$. Using these definitions, p_{ss} for potential flows, and the fact that $F = \langle U\rangle - TS$, it follows that $F = F^* - \langle\chi\rangle$. We note that this relationship holds for any

system where the potential energy is not an explicit function of the control parameter.

APPENDIX B: BROWNIAN DYNAMICS SIMULATIONS

The equation of motion modeling the behavior of polymeric systems in flow is described by the Langevin equation in the absence of inertia. Nonequilibrium trajectories of polymer conformations in flow were simulated by a highly efficient semi-implicit predictor-corrector algorithm.[32] The relevant coordinate of interest is the polymer (or spring) vector. We numerically solve the Langevin equation for the spring vectors yielding a dimensionless stochastic differential equation such that

$$\mathrm{d}\mathbf{x}_k = \left[Pe(\boldsymbol{\kappa}\cdot\mathbf{x}_k) + \frac{1}{4}\left(\mathbf{F}^{spr}_{k-1} - 2\mathbf{F}^{spr}_{k} + \mathbf{F}^{spr}_{k+1}\right)\right]\mathrm{d}t + \sqrt{\frac{1}{2}}(\mathrm{d}\mathbf{W}_{k+1} - \mathrm{d}\mathbf{W}_k), \tag{B1}$$

where $\mathbf{x}_k$ is end-to-end vector of spring k, $\kappa_{ij} = \delta_{i1}\delta_{j1} - \delta_{i2}\delta_{j2}$ is the dimensionless velocity gradient tensor for a planar extensional flow, $\mathbf{F}^{spr} = \nabla_k U$ is the spring force, dt is the time step, d$\mathbf{W}$ represents a Wiener process whose components are chosen from a real-valued Gaussian distribution with mean 0 and variance dt (see the supplementary material[39] text for algorithm details). At each time step, an updated value of $\mathbf{x}_k$ is computed, noting that Pe (and therefore, $Wi = Pe\tilde{\tau}_R$) varies systematically in time as described in the main text. Based on $\mathbf{x}_k$, $\boldsymbol{\kappa}$, and the expression for χ, the work w done on the system (polymer in flow) due to the nonequilibrium transition is calculated. For a transition between any two states, the total work w done is computed and analyzed over a broad range of transition rates. DNA is modeled as a free-draining polymer, which is appropriate for this approach because the analytical form of the steady-state distribution function is well-known and satisfies the condition for which Eq. (5) is valid.[28] Furthermore, the potentials (U and χ) that contribute to the distribution are also well established from theory and experiments.[28,46]

APPENDIX C: CALCULATION OF WORK AND FLOW ENERGY, $-\langle\chi\rangle$

In order to determine the work and corresponding energies for flowing polymer solutions, we determine χ from the configurational distribution function. In this work, we treat a polymer molecule as beads connected by massless springs. In potential flows, the distribution function for a dumbbell is given as, $p_{ness} = Z^{-1}_{ness}\exp[-\beta U(\mathbf{x}) + \frac{1}{4}\beta\zeta\boldsymbol{\kappa}:\mathbf{xx}]$, where $\mathbf{x}$ is the end-to-end vector of a polymer chain, ζ is the drag coefficient of a bead, and $\boldsymbol{\kappa}$ is the velocity gradient tensor that describes the imposed flow field.[28] A planar extensional flow consists of an axis of extension and an orthogonal axis of fluid compression. For this flow, the potential $\chi = -\frac{1}{4}\dot{\epsilon}\zeta(x_1^2 - x_2^2)$, where 1(2) represents the extensional (compressional) axis, and $\dot{\epsilon}$ is the strain rate. In this way, the system is defined as a single polymer in flow, and the flow rate Wi is the control parameter that defines the NESS of the system. As a result, during a finite protocol, work is done on the system when transitioning from Wi_1 to Wi_2, where work is defined by Eq. (6) with $f \equiv Wi$. Finally, the work definition presented in Eq. (6) is similar to those previously considered elsewhere for systems described by Hamiltonian dynamics.[47] Interestingly, based on the steady-state average $\langle\cdot\rangle$ in Eq. (6), it is clear that the system is required to "relax" to the new steady-state in order to completely determine the work done due to the transition. We note that this is in contrast to equilibrium states, where equilibration or relaxation of the final steady-state is not required for the application of the generalized JE.

APPENDIX D: SINGLE MOLECULE FLUORESCENCE MICROSCOPY

Single polymer imaging was performed using lambda DNA (New England Biolabs). dsDNA (6.35 pM) was stained in the presence of 0.4 μM YOYO-1 fluorescent dye (Molecular Probes) for approximately 1 h in the dark, as previously described.[8,35] We directly visualized polymer molecules using epiflourescence microscopy.[41] Lambda DNA was imaged using an Olympus IX71 inverted microscope with a 100× oil immersion objective lens (Olympus UPlanSApo) and an Andor Ixon EMCCD camera. A solid state laser (CrystaLaser) was used as an illumination source at a wavelength of 488 nm. Polymers were imaged in viewing solution containing 50 mM Tris/Tris-HCl (pH 8.0), 1 mM EDTA, 500 mg/ml glucose, 20 mM NaCl, 62.5% sucrose by weight. In order to reduce photobleaching and photocleaving of the YOYO-1 dye, we added β-mercaptoethanol (140 mM), glucose oxidase (65 U/ml), and catalase (1.1 kU/ml) to serve as oxygen scavenging agents. For viewing, $\sim$ 1 ng of flourescently labelled dsDNA was added to 1.7 ml of viewing solution (yielding approximately 1–10 fM dsDNA). Individual dsDNA were visualized in a planar extensional flow generated in a PDMS-based microfluidic device, and images were processed and analyzed using custom codes in IDL and ImageJ software.

APPENDIX E: WORK ANALYSIS FOR SINGLE MOLECULE EXPERIMENTS

In order to determine the work done by the fluid on the polymer from experimental data, we determined χ using the imposed strain rate $\dot{\epsilon}$, drag coefficient ζ, and the molecular stretch in the extensional axis x_1. The strain rate $\dot{\epsilon}$ was determined from particle image velocimetry and a steady-state extension master curve for λ-DNA in an extensional flow. ζ was determined from the longest polymer relaxation time τ_R, which was obtained from an exponential fit to decaying molecular stretch trajectories following the cessation of flow. From theory and simulations of dsDNA, it follows that $\tau_R = 0.9\lambda_H = 0.9\zeta\beta Nb^2/12$, where $N = 159$ is the number of Kuhn segments in the polymer, and $b = 132$ nm is the Kuhn segment length.[25] Based on this relationship, ζ can be computed directly from τ_R. x_1 was determined from epifluorescence microscopy. We use only x_1 in our analysis because beyond the coil-stretch transition (our region of interest) $x_1 \gg x_2$.

[1] I. Prigogine, Science **201**, 777 (1978).
[2] Y. Oono and M. Paniconi, Prog. Theor. Phys. Suppl. **130**, 29 (1998).

[3]T. Hatano and S.-I. Sasa, Phys. Rev. Lett. **86**, 3463 (2001).
[4]J. R. Prakash and R. A. Mashelkar, J. Non-Newton. Fluid Mech. **40**, 337 (1991).
[5]A. B. Marciel, M. Tanyeri, B. D. Wall, J. D. Tovar, C. M. Schroeder, and W. L. Wilson, Adv. Mater. **25**, 6398 (2013).
[6]C. Rangel-Nafaile, A. B. Metzner, and K. F. Wissbrun, Macromolecules **17**, 1187 (1984).
[7]P.-G. de Gennes, J. Chem. Phys. **60**, 5030 (1974).
[8]C. M. Schroeder, H. P. Babcock, E. S. G. Shaqfeh, and S. Chu, Science **301**, 1515 (2003).
[9]G. Marrucci, Trans. Soc. Rheol. **16**, 321 (1972).
[10]H. C. Booij, J. Chem. Phys. **80**, 4571 (1984).
[11]N. J. Wagner, H. C. Öttinger, and B. J. Edwards, AIChE J. **45**, 1169 (1999).
[12]M. Grmela and H. C. Öttinger, Phys. Rev. E **56**, 6620 (1997).
[13]D. Jou, J. Casas-Vazquez, and M. Criado-Sancho, *Thermodynamics of Fluids Under Flow*, 2nd ed. (Springer, Dordrecht, Netherlands, 2011).
[14]C. Baig, V. G. Mavrantzas, and H. C. Öttinger, Macromolecules **44**, 640 (2011).
[15]U. Seifert, Rep. Prog. Phys. **75**, 126001 (2012).
[16]G. E. Crooks, Phys. Rev. E **60**, 2721 (1999).
[17]D. J. Evans, E. G. D. Cohen, and G. P. Morriss, Phys. Rev. Lett. **71**, 2401 (1993).
[18]C. Jarzynski, Phys. Rev. Lett. **78**, 2690 (1997).
[19]G. Hummer and A. Szabo, Proc. Natl. Acad. Sci. U.S.A. **98**, 3658 (2001).
[20]J. Liphardt, S. Dumont, S. B. Smith, I. Tinoco, and C. Bustamante, Science **296**, 1832 (2002).
[21]A. N. Gupta, A. Vincent, K. Neupane, H. Yu, F. Wang, and M. T. Woodside, Nat. Phys. **7**, 631 (2011).
[22]E. H. Trepagnier, C. Jarzynski, F. Ritort, G. E. Crooks, C. J. Bustamante, and J. Liphardt, Proc. Natl. Acad. Sci. U.S.A. **101**, 15038 (2004).
[23]S. Park, F. Khalili-Araghi, E. Tajkhorshid, and K. Schulten, J. Chem. Phys. **119**, 3559 (2003).
[24]S. Toyabe, T. Sagawa, M. Ueda, E. Muneyuki, and M. Sano, Nat. Phys. **6**, 988 (2010).
[25]F. Latinwo and C. M. Schroeder, Soft Matter **10**, 2178 (2014).
[26]F. Latinwo and C. M. Schroeder, Macromolecules **46**, 8345 (2013).
[27]D. A. Sivak and G. E. Crooks, Phys. Rev. Lett. **108**, 150601 (2012).
[28]R. B. Bird, C. F. Curtis, R. C. Armstrong, and O. Hassager, *Dynamics of Polymeric Liquids*, 2nd ed. (Wiley, New York, 1987), Vol. 2.
[29]In this article, we use order and control parameters interchangeably.
[30]*Free Energy Calculations: Theory and Applications in Chemistry and Biology*, Springer Series in Chemical Physics Vol. 86, edited by Ch. Chipot and A. Pohorille (Springer-Verlag, Berlin, 2007).
[31]D. Wales, *Energy Landscapes: Applications to Clusters, Biomolecules and Glasses*, 1st ed., Cambridge Molecular Science (Cambridge University Press, 2004).
[32]M. Somasi, B. Khomami, N. J. Woo, J. S. Hur, and E. S. G. Shaqfeh, J. Non-Newton. Fluid Mech. **108**, 227 (2002).
[33]R. M. Jendrejack, J. J. de Pablo, and M. D. Graham, J. Chem. Phys. **116**, 7752 (2002).
[34]R. G. Larson, T. T. Perkins, D. E. Smith, and S. Chu, Phys. Rev. E **55**, 1794 (1997).
[35]T. T. Perkins, D. E. Smith, and S. Chu, Science **276**, 2016 (1997).
[36]D. R. Tree, A. Muralidhar, P. S. Doyle, and K. D. Dorfman, Macromolecules **46**, 8369 (2013).
[37]C. M. Schroeder, E. S. G. Shaqfeh, and S. Chu, Macromolecules **37**, 9242 (2004).
[38]F. Latinwo and C. M. Schroeder, Soft Matter **7**, 7907 (2011).
[39]See supplementary material at http://dx.doi.org/10.1063/1.4900880 for characteristic scales, supporting text, and figures.
[40]M. Tanyeri and C. M. Schroeder, Nano Lett. **13**, 2357 (2013).
[41]C. Brockman, S. J. Kim, and C. M. Schroeder, Soft Matter **7**, 8005 (2011).
[42]For λ-DNA described by the Marko-Siggia force-relation, $\beta U = Ll_p^{-1}\left[0.5\,(x/L)^2 - 0.25\,(x/L) + 0.25(1 - x/L)^{-1}\right]$, where L is the contour length of the molecule, x is the end-to-end distance, and l_p is the persistence length.
[43]To calculate work and the effective free energy for freely draining multi-bead-spring chains, we used $\chi = -\frac{\zeta}{2}\boldsymbol{\kappa} : \sum_i \sum_j C_{ij}\mathbf{x}_i\mathbf{x}_j$, where C_{ij} is the Kramer's matrix and i and j represent the indices of the connector vectors.
[44]M. Süzen, M. Sega, and C. Holm, Phys. Rev. E **79**, 051118 (2009).
[45]D. Asenjo, F. Paillusson, and D. Frenkel, Phys. Rev. Lett. **112**, 098002 (2014).
[46]J. F. Marko and E. D. Siggia, Macromolecules **28**, 8759 (1995).
[47]S. R. Williams, D. J. Searles, and D. J. Evans, Phys. Rev. Lett. **100**, 250601 (2008).